Experimental Analysis of Dynamic Charge Acceptance Test Conditions for Lead-Acid & Lithium Iron Phosphate Cells

M J Smith*, D T Gladwin, D A Stone

Electrical Machines and Drives Research Group,
Department of Electronic and Electrical Engineering,
The University of Sheffield,
Solly Street, Sheffield, S1 4DE, UK

Abstract

This paper presents the results of a series of tests to determine the Dynamic Charge Acceptance (DCA) performance of small form-factor carbon-enhanced VRLA cells designed for use in Hybrid Electric Vehicle (HEV) applications, together with standard lead-acid and lithium iron phosphate (LFP) cells. The results demonstrate how varying the conditions and parameters of the standard DCA test regime can provide a superior evaluation of DCA performance and lead to a better understanding of cell behaviour under real-world conditions. A modified test procedure is proposed, based on the DCA Short Test profile (EN50342-6). Results are presented for a batch of carbon-enhanced cells, tested at various temperatures, rest periods and States of Charge (SoC) for the cell. These conditions having been chosen to mimic a range of real-life scenarios which could potentially be encountered during HEV operation. The resulting analysis demonstrates clear variations and trends in DCA performance which may be used to inform conditions for future testing regimes. The modified test procedure is then applied to standard lead-acid and LFP 26650-type cells and the results compared.

Keywords: Automotive battery; Carbon-enhanced lead-acid; Dynamic charge acceptance; Hybrid Electric Vehicle; Lithium iron phosphate; Test regime

2017 MSC: 00-01, 99-00

1. Introduction

Recent years have seen battery technology and performance become increasingly important in automotive applications. Driven by a desire to reduce emissions and rises in fuel costs, the function of automotive batteries has shifted from an auxiliary power source to providing significant contributions to the performance of the vehicle; particularly in the case of fully electric vehicles (EV), where it is the only source of energy. This, coupled with increasingly power-hungry driver-

---

*Corresponding author
Email address:* `matt.j.smith@sheffield.ac.uk` (M J Smith)

aids, entertainment and HVAC systems is making it ever more important that the behaviour of automotive batteries be well understood.

1.1. Battery Use in Vehicles

In traditional internal-combustion (IC) engined vehicles the battery is used exclusively as an auxiliary energy store for when the engine is switched off, once running the engine provides all power for the vehicle, both mechanical via the drive-train and electrical via the alternator. In this configuration the battery is subject to infrequent, short discharges at high currents (around 16 times the 1-hour rate, C_1) when starting the engine, followed by modest recharging to full state-of-charge (SoC) at around 1 C_1 from the alternator [1]. The use of automotive batteries for starting, lighting and ignition (SLI) and their failure modes under these conditions is well understood.

An increasingly common modification to this method of working is the stop-start system. Here the IC engine is stopped automatically when the vehicle is stationary, and re-started before moving off. This system is designed to reduce the time the engine spends running whilst the vehicle is stationary, thus reducing fuel usage and emissions. Whilst this imposes a more demanding duty on the batteries due to the increased frequency of the discharge-charge cycles experienced by the battery, the fundamental operating mode and recharging mechanism remains the same.

More significant changes to battery operation are imposed by hybrid electric vehicles (HEV). In such vehicles the IC engine is used in conjunction with the batteries such that both provide traction power. There are several configurations possible for the drive arrangement of such vehicles [2], but the principle of operation is similar; the vehicle may be driven by either the engine or batteries alone, or by the two together. This allows such vehicles to drive quietly and with zero emissions at low speeds, such as within cities. It also means they can be fitted with smaller, more efficient IC engines sufficient for most driving, but maintain performance when accelerating by using their batteries to increase available power.

As the batteries are by necessity much larger in a HEV than in a conventional vehicle, an alternator is not sufficient to recharge them. Therefore recharging is performed by using the electrical machine fitted within the drive-train as a generator [2]. This allows the batteries to be recharged by the IC engine through the drive system, but also allows energy to be stored in the batteries when the vehicle brakes.

This modifies significantly the loads imposed on the battery. Aside from the large discharges associated with starting the IC engine, there are additional discharge spikes caused by acceleration as well as longer periods of lower discharge currents where the vehicle is running in purely electric mode. The charging profile is similarly modified, the batteries are no longer steadily charged back to full SoC, instead operation is often at partial SoC. Charging from the engine is controlled to a modest rate, but is interspersed with large charge spikes due the regenerative braking system;

these spikes can reach up to 30 C_1 under heavy braking [1]. The operation of batteries under these conditions of high-rate partial-state-of-charge (HRPSoC) is becoming increasingly common as the number of HEV's increases.

1.2. Charge Acceptance

It can be seen from the above that to maximise the effectiveness of the HEV drive-train, as much energy as possible must be recaptured and stored during any and all regenerative braking periods. The main factor limiting the ability to capture this energy is the charge acceptance of the batteries at HRPSoC. As the batteries used in automotive applications are being required to provide more of the electrical power to the vehicle it is crucial that they are able to be recharged sufficiently quickly and that the performance of batteries under these conditions is known. To this end numerous testing methodologies have been developed to characterise the performance of automotive batteries, from stand-alone tests such as Dynamic Charge Acceptance (DCA) and Hybrid Pulse Power Characterisation (HPPC) to full simulated drive-cycle tests like NEDC and WLTP.

Understanding the DCA performance of automotive batteries has been identified as a key requirement for the development of electric vehicles [3, 4, 5], and standard test procedures have been designed to characterise the DCA performance of batteries [6]. This paper presents the results of an investigation into how varying the conditions and parameters of the standard DCA test regime can provide a superior evaluation of DCA performance and lead to a better understanding of the behaviour of the cell under real world conditions.

2. DCA Overview

DCA is a measure of the charge efficiency of a battery, the higher the DCA value the better the charge efficiency. The standard test for determining DCA performance involves the application of a defined current waveform to the battery under test, the response of the battery to this waveform is used to calculate DCA performance.

2.1. Microcycling

At the heart of the DCA test is the microcycle, it is this which defines the current applied to the battery, and from which the performance may be determined. The standard microcycle, as defined by the European Standard DCA Test A3 specification (EN 50342-6) [6] is given in Figure 1a, this is summarised in tabular form below.

3

Step	Description
1, (A – B)	Charge at 1.67 A·Ah^{-1} with voltage limit of 2.47 V per cell for 10 s
2, (B – C)	Rest 30 s
3, (C – D)	Discharge at 1.00 A·Ah^{-1} until charge added in Step 1 is removed
4, (D – E)	Rest 30 s

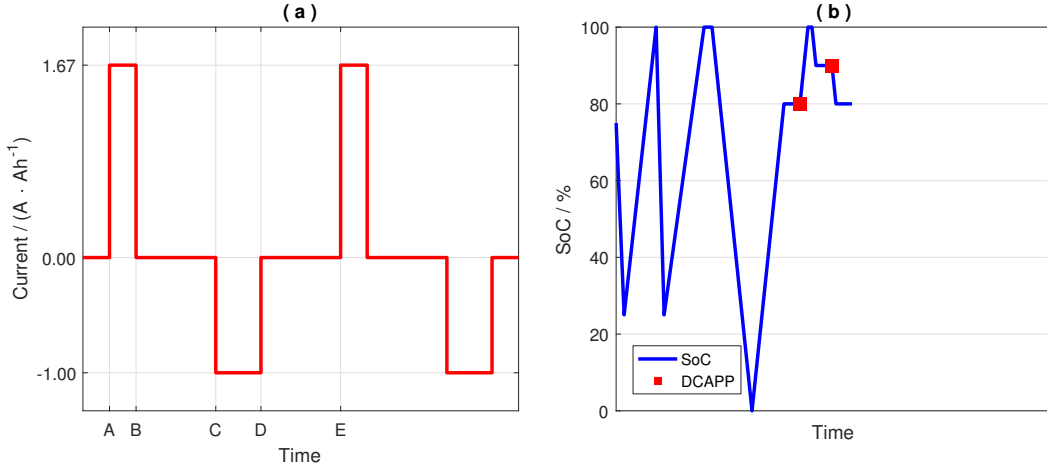Table 1: Standard DCA Test A3 Microcycle Current Profile Procedure

Figure 1: DCA Test A3 Profiles. (a) Microcycle Current Profile (A – E), (b) SoC Profile & DCAPP Locations

DCA performance is determined by the response of the battery to the charge phase of the microcycle (step 1). During this phase the test procedure attempts to charge the battery with a current of 1.67 A·Ah^{-1} for 10 seconds, this will cause the terminal voltage of the battery to rise. If during the charge step the voltage reaches the set limit of 2.47 V per cell (equivalent to 14.8 V for a standard 6 cell battery) the charge current is reduced to maintain the battery at the voltage limit; a reduction in charge current equates to a reduction in the charge accepted by the battery. DCA is thus determined by the difference in the amount of charge accepted by the battery compared to the total available from the charge pulse. All currents used during the microcycle are normalised to the capacity of the battery (C_{exp}), which is obtained experimentally during the test procedure.

Microcycles are applied to the battery in blocks of 20 to form a DCA Pulse Profile (DCAPP). Each microcycle and hence each DCAPP, is inherently energy-balanced. The amount of charge removed during the discharge in step 3 is equal to that accepted by the cell during the charge step, i.e:

$$\int_A^B I(t)\ dt = -\int_C^D I(t)\ dt \tag{1}$$

This ensures that the SoC of the battery does not change between microcycles, and therefore does not drift during the course of the DCAPP. Note that this assumes equal efficiencies for both

4

charge and discharge, in practice the difference between these efficiencies will have little effect due to the small energy throughput and the tests being conducted away from the extremes of SoC; this assumption is also implicit in the A3 test specification.

2.2. Standard DCA Test A3 Procedure

Figure 1b shows the SoC profile and DCAPP locations as specified by the standard DCA test procedure. The test begins with two heavy discharges to test the reserve capacity performance of the battery, each followed by full recharge to 100% SoC. The battery capacity, C_{exp}, is then determined by a standard-rate discharge to a minimum voltage of 1.75 V per cell. After this preconditioning the battery is recharged to 80% SoC where the first DCAPP is performed, this tests the DCA performance of the battery with charge history, i.e. after having been previously subjected to charging. The battery is then fully charged before being discharged to 90% SoC for a second DCAPP, this time testing with discharge history. The test then continues to perform various configurations of simulated drive-cycles, but these are outside the scope of this paper. Throughout the entirety of the test, the battery is maintained at an ambient temperature of 25°C.

2.3. DCA Calculation

DCA is generally expressed as the average recuperation current (I_{recu}), in units of A·Ah^{-1} [5], for the time of the charge pulse. Thus, for a pulse of arbitrary length, DCA is given by

$$I_{recu} = \frac{Ah_{recu} \cdot 3600}{C_{exp} \cdot t} \tag{2}$$

where Ah_{recu} is the amount charge accepted during the pulse in ampere-hours, C_{exp} is the capacity of the battery in ampere-hours and t is the length of the pulse in seconds.

The DCA Test A3 calculates I_{recu} from the average current of all 20 charge pulses in the DCAPP. As both the length and number of pulses are specified (as 10 seconds and 20 pulses respectively), this allows for the simplification of (2)

$$I_{recu} = \frac{\left(\sum\limits_{n=1}^{20} Ah_{recu}(n) \right) \cdot 18}{C_{exp}} \tag{3}$$

3. Experimental Setup

All the testing described herein was conducted using a MACCOR Series 4000 automated test system. This allows for the complete test procedure to be pre-programmed into the tester and run on demand. The system logs, in high-resolution, all important parameters (current, voltage, temperature, etc) during the running of the test, this data is then analysed to provide the results presented here.

Coupled to the testing equipment are environmental chambers, in which the tested cells are placed. These chambers are programmable and capable of both cooling and heating, to ensure the tested cells are maintained in known and controlled environmental conditions for the duration of the testing.

4. Test Procedure Modifications

120 The standard DCA Test A3 is somewhat limited in its ability to characterise the DCA performance of batteries as it only performs DCA analysis at two points, both with similar SoC levels. As DCA performance is critical to HEVs and the batteries in HEV applications are likely to be cycled across a wide range of SoC it is important that DCA performance be measured across a similarly wide range. To this end, it is necessary to modify the standard test procedure to bet-
125 ter match these requirements. The testing described below was performed using small form-factor 6 Ah carbon-enhanced VRLA cells, of an experimental prismatic construction specifically designed for HEV applications [7] and manufactured by Banner GmbH. Prior to this testing they were used to evaluate the performance of the design and were known to be in good condition.

4.1. Modified SoC Profile

130 The modified SoC profile is given in Figure 2, this addresses the shortcomings discussed above. The principal differences are the locations of the DCAPP and the SoC at which they are performed. In this profile DCA is measured in 10 places and five SoC across the SoC range, the effects of charge and discharge history are also considered by measuring the DCA at the same SoC with both charge and discharge history. The range of SoC over which the measurements take place are
135 intended to assess DCA performance over a range similar to that of an HEV.
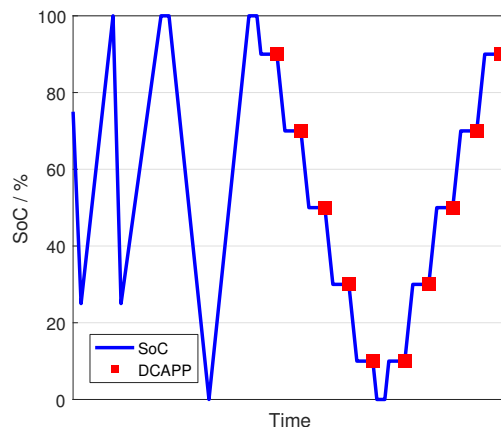

Figure 2: Modified DCA Test SoC Profile & DCAPP Locations

6

4.2. Modified DCA Calculation

To better assess the performance of the cells tested, the DCA has been calculated for each charge pulse within the DCAPP, which allows for any trends present during the DCAPP to be identified. To this end the DCA is calculated using a modified form of (2). Given that the length of the charge pulse is known to be 10 s, the calculation may be simplifed to give

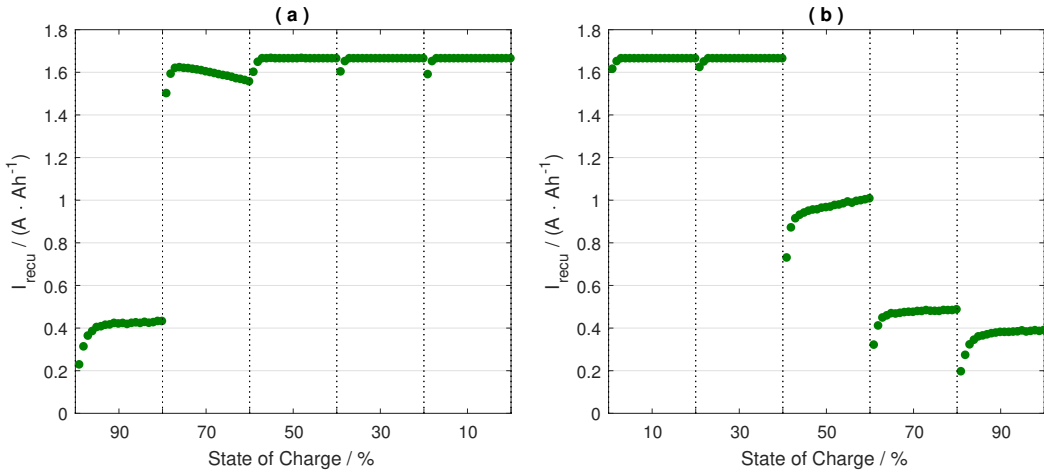$$I_{recu} = \frac{Ah_{recu} \cdot 360}{C_{exp}} \tag{4}$$

Figure 3: DCA Analysis Result at 25°C, Modified SoC Profile. (a) with Discharge History, (b) with Charge History

Figure 3 shows the typical result of the DCA analysis obtained from the modified test procedure. Before beginning any discussion of the results, it seems wise to briefly describe the figures used to present said results. The abscissa is divided into five discrete sections, one for each SoC of the test procedure. Within each section are plotted the DCA results for each microcycle, thus each section contains 20 individual data-points, these data-points are arranged chronologically from left to right. Two plots are provided showing the results of the testing with both charge and discharge history.

It may be seen from Figure 3 that the modified test profile provides far more information regarding the DCA performance across a range of SoC. Despite this however there is a clear limitation imposed by charge current used, it may be seen that at many of SoC examined the cell is capable of accepting all the charge available and thus the result is artificially limited to the maximum charge current of 1.67 A·Ah^{-1}.

4.3. Increased Charge Current

To overcome the limitation discussed above, the microcycle profile is modified to increase the current during the charge (step 1) to 4.00 A·Ah^{-1}. This value more closely matches the charge currents likely to be experienced by HEV batteries, whilst avoiding excessive stressing of the

cells. All other parameters of the microcycle profile remain as indicated in Figure 1a and Table 1. Figure 4 shows the results following these modifications.
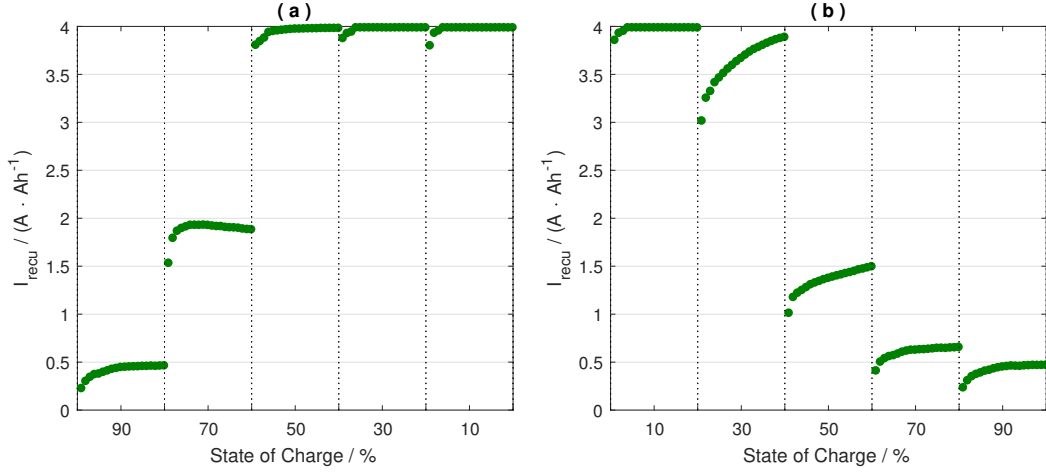

Figure 4: DCA Analysis Result at 25°C, Modified Microcycle Profile and Increased Charge Current. (a) with Discharge History, (b) with Charge History

These results show much more clearly the trend in DCA performance with varying SoC and charge history. The most obvious feature is the variation in DCA with SoC, in broad terms DCA improves with reducing SoC. This is to be expected as the charge capacity of a battery is finite and the further below this limit the present capacity, the more readily charge will be accepted. In this case SoC is analogous to current battery capacity.

By calculating the DCA result for every microcycle, trends within the DCAPP become apparent. In this case there is generally a significant increase in the level of charge acceptance between the first and second pulses, which then reduces as the DCAPP progresses although the general trend of increasing DCA continues. This is more particularly pronounced at lower SoC.

It can also be seen that there are differences in DCA at the same SoC caused by the charge history of the cell. Whilst the results at 90 % SoC correlate well, at all SoC below this, tests with discharge history show significantly improved DCA results. This behaviour has previously been observed in lead-acid batteries when subjected to the standard DCA test and similar profiles [5, 8].

This result clearly indicates that DCA performance is not merely governed by the SoC of the cell at the time of testing, the electrochemical processes occurring within the cell also affect the results. All testing was carried out following a 1-hour rest period to allow these processes to reach an equilibrium. Despite the rest however, the effect of charge history remains significant, thus it must also be considered as a fundamental factor when assessing DCA performance.

4.4. Rest Period Variation

Whilst the 30 s rest period specified by the A3 test is fine for determining DCA performance and is necessary for defining a standard test, in real-world applications the rest periods between charge pluses are likely to vary considerably. To assess the effect of this variation on the test cells the microcyle was further modified by altering the length of the rest periods used (steps 2 & 4). These were both increased and decreased by one order of magnitude to test cell performance with rest periods of 300 s, 30 s and 3 s; Figures 5a & 5b show the results from this testing.

In this case, the most general observation is that charge acceptance is indeed affected by the rest period. Shorter rests improve DCA performance. It is also apparent that the rest period affects the way charge acceptance changes throughout the DCAPP. With short rest periods the charge acceptance increases more rapidly during the initial pulses before beginning to plateau, as the rest period is increased, however, this takes longer to occur. There is also one isolated case (at 70% SoC with discharge history) where the longest rest period led to a significant decrease in charge acceptance over the DCAPP.

To better illustrate the variations caused by charge history, the results were recalculated using the DCA Test A3 method, as given by (3). This produces a single, average DCA value for each DCAPP allowing charge history to be more easily compared. Figure 5c shows the result of this recalculation for the 30 s rest period, clearly showing the effects of charge history, revealing the hysteresis-like behaviour resulting from this influence. The greatest variation lies within the mid-SoC range, which is the typical range of operation of a HEV battery; thus indicating the need to properly analyse the behaviour of such batteries under these conditions if their real-world performance is to be assessed.

Considering the average charge acceptance for the other rest periods, shown in Figure 5d, again the effects of charge history are apparent, with the behaviour previously observed being exhibited regardless of rest period. It may also be seen that the effect of the rest period is broadly consistent across the SoC range. This is a very useful result, as in real-world applications the rest period between charge pulses is likely to vary significantly, this shows that such variation does not have as significant effect on DCA performance as other factors, such as SoC.

Although charge history continues to have a large influence, there is much greater differentiation between rest periods for those results with discharge history. When the cell has charge history however, there is very little difference between the 30 s and 3 s rest periods in either start and end points or shape of the result. This is interesting and suggests that whilst DCA performance is poorer when the cell has charge history, it is also more consistent with regards to rest period.
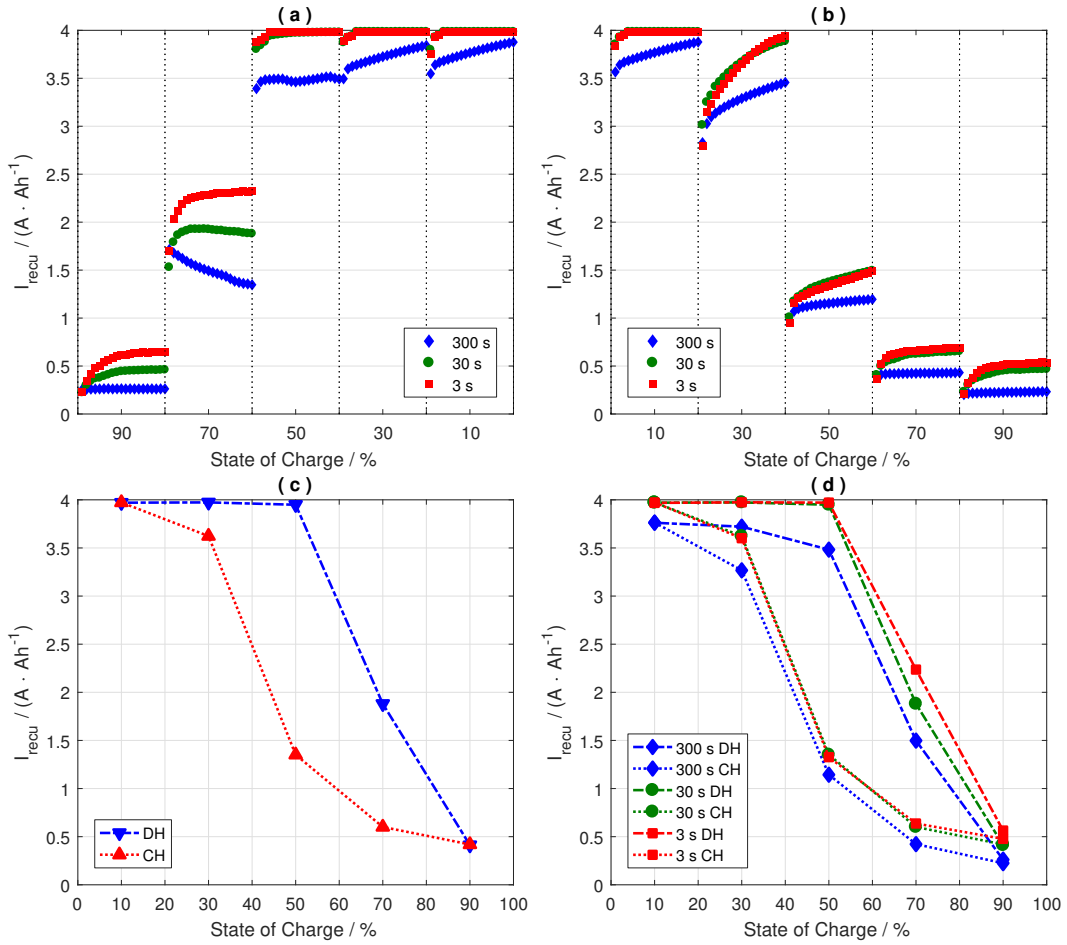
Figure 5: DCA Analysis Result, Variation with Rest Period at 25°C. (a) with Discharge History, (b) with Charge History, (c) Average Charge Acceptance Variation with 30 s Rest Period, (d) Average Charge Acceptance Variation for all Rest Periods

4.5. Temperature Variation

As with rest period it is necessary for the A3 Test to fix the ambient temperature during testing to 25°C, in order to define a repeatable standard. However, in practice this will not be the case, instead the batteries in HEVs are subject to significant variations in ambient temperature during their operation. To test performance across a range of temperatures, the test procedure was repeated with the cell at an ambient temperature of -10, 0, 10, 25, or 40°C. These temperatures were chosen to best represent the likely real-world conditions HEV batteries may be exposed to.

Prior to testing the cell was maintained at the test temperature for a period of 24 hours to allow the internal temperature to equalise to that of the ambient. One complete test was then performed before the ambient temperature was adjusted and the cell was again allowed time to equalise. Figures 6a & 6b show the results of this analysis, using the standard rest period of 30 s.

The general trends in the shape of the charge acceptance throughout the DCAPP and the
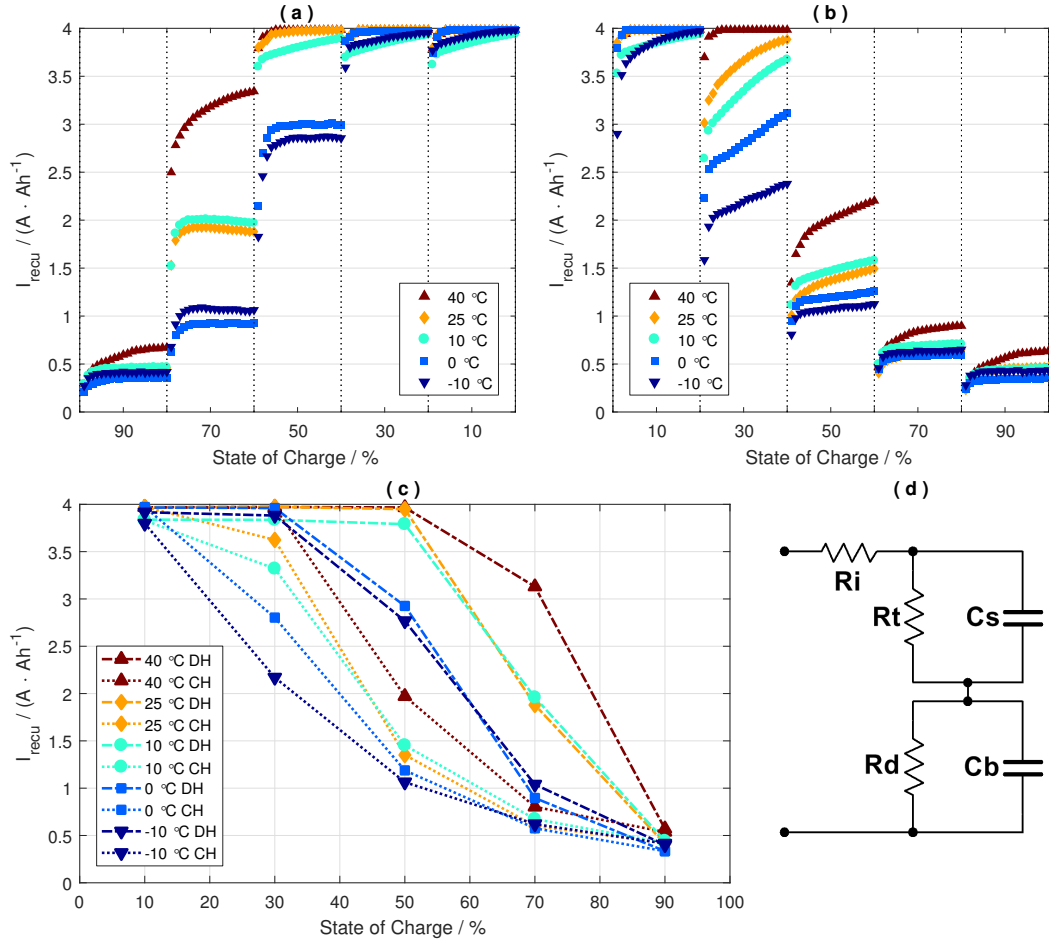
Figure 6: DCA Analysis Result, Variation with Temperature with 30 s Rest Period. (a) with Discharge History, (b) with Charge History, (c) Average Charge Acceptance, (d) Randles' Cell Equivalent Circuit

effects of charge history are again present as previously discussed, the major interest here is the significant worsening of DCA performance as temperature decreases. It is well known that the capacity of batteries is reduced as temperature decreases, but the DCA test measures the capacity of the battery at the beginning of the procedure and scales the charge pulses appropriately, so this alone cannot explain the results observed.

The charge storage mechanism within the cell is usually modelled electrically as a pair of series connected capacitors, this equivalent circuit representation is known as the Randles' Model [9] as shown in Figure 6d. From the Randles' Model, R_d represents the self discharge resistance of the cell and R_i the resistance of the cell's internal connections, of most interest in this case are C_b, C_s and R_t. C_b is the main charge storage element of the cell, whilst C_s and R_t together model the transient effects of ion concentrations and current densities on the cell plates. C_s is typically several orders of magnitude smaller than C_b [10].

The short-duration, high-current nature of the DCA charge pulse makes it primarily a test

11

of the surface capacitance of the cell. In fact, the DCA profile shares many similarities with a Pseudo-random Binary Sequence (PRBS) profile, which has been shown to be a good indicator to the values of the discreet components comprising the Randles' model [11]. This testing also showed a significant drop in the value of C_s as temperature is decreased. Clearly a reduction in the surface capacitance will translate into a reduction in the ability of the cell to accept charge.

The reduction in temperature will also affect the value of C_b. This is to be expected as the electrochemical processes with the battery, modelled by C_b, are governed by the Arrhenius equation [12]. The Arrhenius equation relates temperature to the rate of a chemical reaction, for example, those occurring within a cell. The equation states that the reaction rate will double for every $10°$C increase in temperature. At lower temperatures the rate of reaction will be slowed, meaning the amount of charge which may be accepted by C_b during the 10 second DCA charge pulse will be reduced [13]. Together these phenomena have the effect of significantly reducing the DCA ability of the cell, as temperature decreases.

Considering the average charge acceptance, Figure 6c reveals an that the hysteresis like behaviour is again present, but the effect of temperature is far more pronounced than that of the rest period, and has the effect of shifting the entire curve downward as temperature decreases. The result of this downward-shift is that at colder temperatures, the results with discharge history begin to look very similar to the results with charge history at higher temperatures. This suggests that the effects of charge history are analogous to those of temperature, with the difference in performance between charge and discharge history being roughly equivalent to the difference in performance associated with a $50°$C change in temperature for these cells. This may be observed by comparing the results at 0 or -$10°$C with discharge history to those at $40°$C with charge history.

5. Comparison with Standard Lead-Acid

The test methodology described above has been shown to yield informative results regarding the DCA performance of carbon-enhanced lead-acid cells across a range of conditions, this methodology has been extended to investigate the performance of standard lead-acid cells under the same conditions. This testing phase used standard lead 2 V, 2.5 Ah, Enersys 'Cyclon' VRLA cells, which were new at the time of testing. The results of the analysis for standard lead-acid are shown in Figure 7. As would be expected they share many similarities with the carbon-enhanced cells, although differences are apparent.

The most obvious difference is in the effect of charge history, this is much more equal for both charge and discharge history, also the trends within each DCAPP exhibit much the same shape (both 30 & 3 s rests being steeper than 300 s) regardless of charge history. It can also be seen that the variation in DCA performance with respect to SoC is more linear for the standard lead than that of the carbon-enhanced. As previously observed DCA is improved with reduced rest periods.

Also apparent is that the reduced effects of charge history come at the expense of DCA performance when the cell has discharge history. It can been seen that for equivalent SoC, with discharge history the DCA performance of standard lead is poorer than that with carbon enhancement.

6. Comparison with Lithium-ion

Following the testing of lead-based chemistries and the useful results yielded, an investigation was performed to see if the test methodology previously described was also applicable to lithium-ion cells. For this phase of testing new Mottcell IFR26650 3.2 V, 3.3 Ah, 26650-type lithium iron phosphate (LFP) cells were used. The only changes made to the test procedure have been to vary the voltage limits used, this is necessary to match the different voltages of the LFP cells. All testing has been performed under environmentally controlled conditions at 25°C. Figure 8 shows the results of these tests.
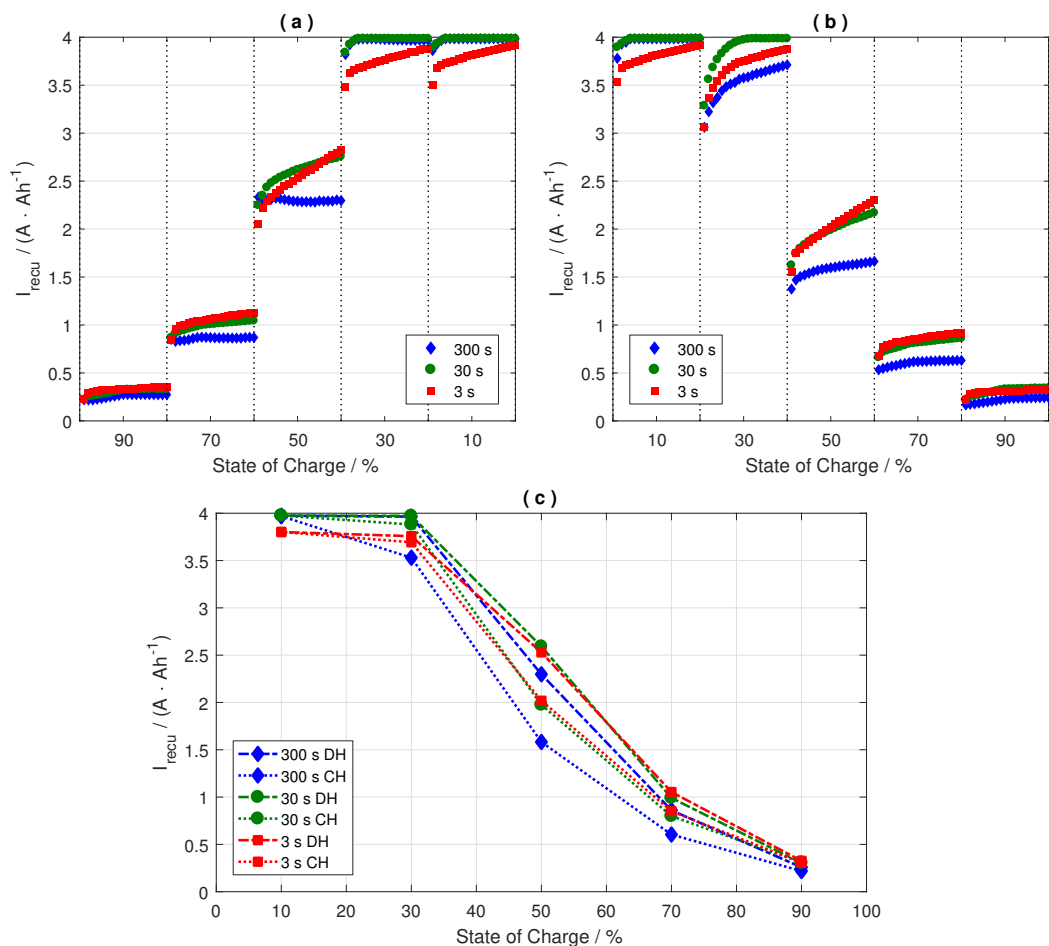

Figure 7: DCA Analysis Result for 2 V, 2.5 Ah standard VRLA cell, 25°C. (a) with Discharge History, (b) with Charge History, (c) Average Charge Acceptance
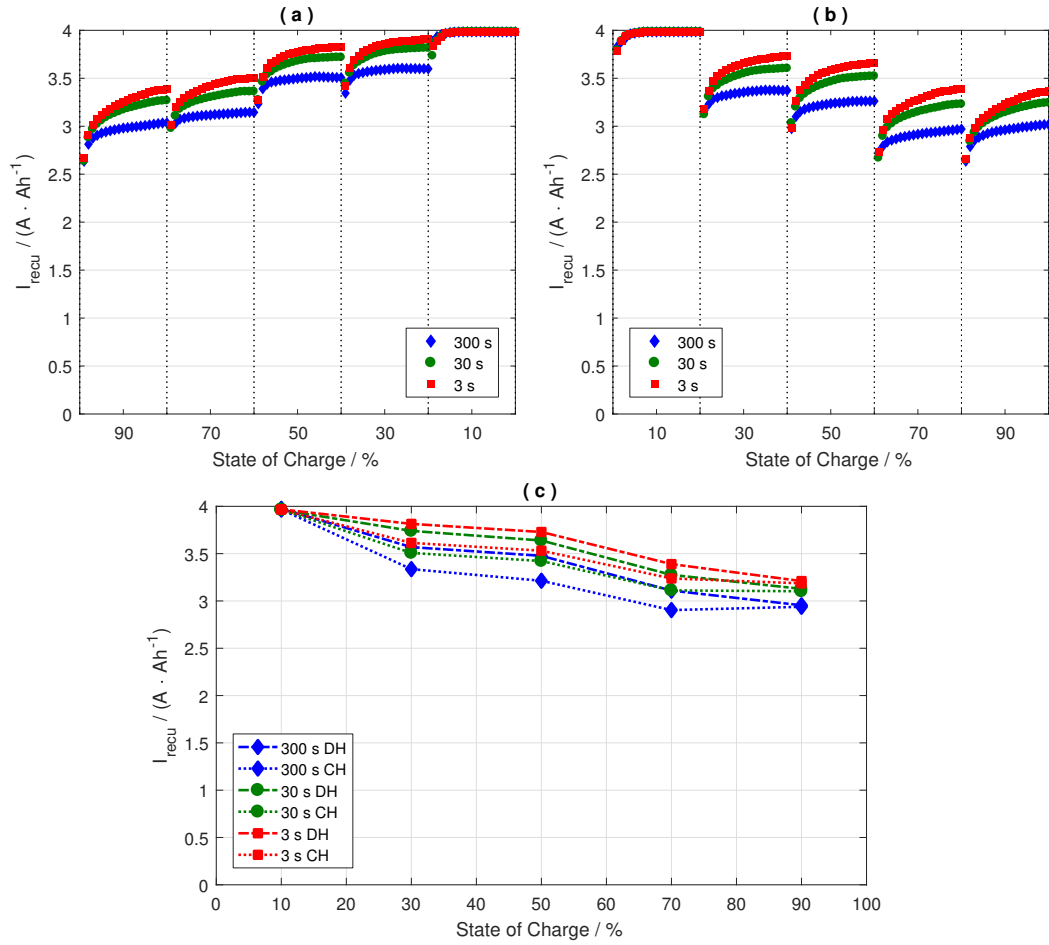
13

Figure 8: DCA Analysis Result for 3.2 V, 3.3 Ah, LiFePO$_4$ cell, 25°C. (a) with Discharge History, (b) with Charge History, (c) Average Charge Acceptance

The LiFePO$_4$ results show significant differences from those observed with lead-based chemistry, although all the trends previously identified are present to some extent. Firstly, variation with charge history is all but eliminated, there is only a very slight reduction in DCA performance when the cell has charge history.

Secondly the effects of SoC are much reduced, making the DCA performance much more consistent across a wide SoC range. The DCA performance is much improved over carbon-enhanced lead at high SoC conditions, however as SoC is reduced carbon-enhanced lead begins to show better performance, particularly below around 30% SoC. It is clear from the results that even if the charge current is increased further, even at 10% SoC the LFP cell would be unlikely to accept more than around 4.5 A·Ah^{-1}. This compares unfavourably to the carbon-enhanced lead which have been shown to accept up to 8 A·Ah^{-1} under similar conditions (see Section 7).

The effects of the rest period are clearly evident, in all cases reduced rest period improves the DCA performance. As with charge history however, the effect is much more consistent and the

14

shapes of the DCAPP remain broadly similar despite the changing rest periods.

These results also indicate that the test methodology described is a useful device for determining the DCA performance of cells with a range of chemistries. It also reinforces the validity of the test and of the trends identified, as these too appear largely independent of the chemistry of the cell investigated.

7. Extended Testing

After the completion of the initial testing with the carbon-enhanced lead-acid cells, and the validation of the results against cells of other chemistries, an additional series of tests were performed to further analyse some interesting features noticed in the results. All these tests were performed using the carbon-enhanced cells.

The first feature of interest is the DCA performance of the cells with higher recuperation currents. The testing thus far had been limited to 4.00 A·Ah^{-1} to avoid excessive stress on the cells, however this places an artificial limit on the results and thus leaves uncertainty over the true capabilities of the cells. To definitively determine this, the tests were repeated with a much increased current limit.

The second area of interest was the effect of the rest period on the DCA performance during the DCAPP, this is most evident in Figure 5a from the results at 70% SoC. Here it can be seen that DCA performance increases slightly across the DCAPP for the test with 3 s rest, whilst it remains broadly flat for the test with 30 s rest, and decreases significantly with 300 s rest. This would seem to be a critical point in terms of SoC where the DCA performance is highly dependant on the rest period, however 20 microcycles are insufficient to draw any sound conclusions, therefore a test was performed with a much increased DCAPP length.

7.1. High Current Testing

The initial testing was performed with a charge current limit of 4.00 A·Ah^{-1}, this has had the effect of artifcially limiting the maximum charge acceptance to this level. To fully understand the performance of the cells, the tests have been repeated with a maximum charge current of 12.00 A·Ah^{-1}, as this is the maximum available from the test equipment. By increasing the limit it is possible to reveal the maximum charge the cells are capable of accepting across the whole range of test parameters. This gives a truer picture of the performance the cells under the typical HRPSoC conditions they are likely to experience in HEV applications. Figure 9 shows the results of this testing.

These results are broadly similar to those previously observed, namely in that increased temperature results in improved DCA performance. Also observed in this case is that the rate of increase in DCA during each DCAPP is increased at higher temperatures this is most pronounced

with long rest periods. It may be seen from Figures 9a & 9b at 0°C, for the tests with 300 s rests, the DCA performance generally falls during the DCAPP, this is in contrast to that of Figures 9e & 9f at 40°C where at 300 s rests the DCA is generally rising or flat.
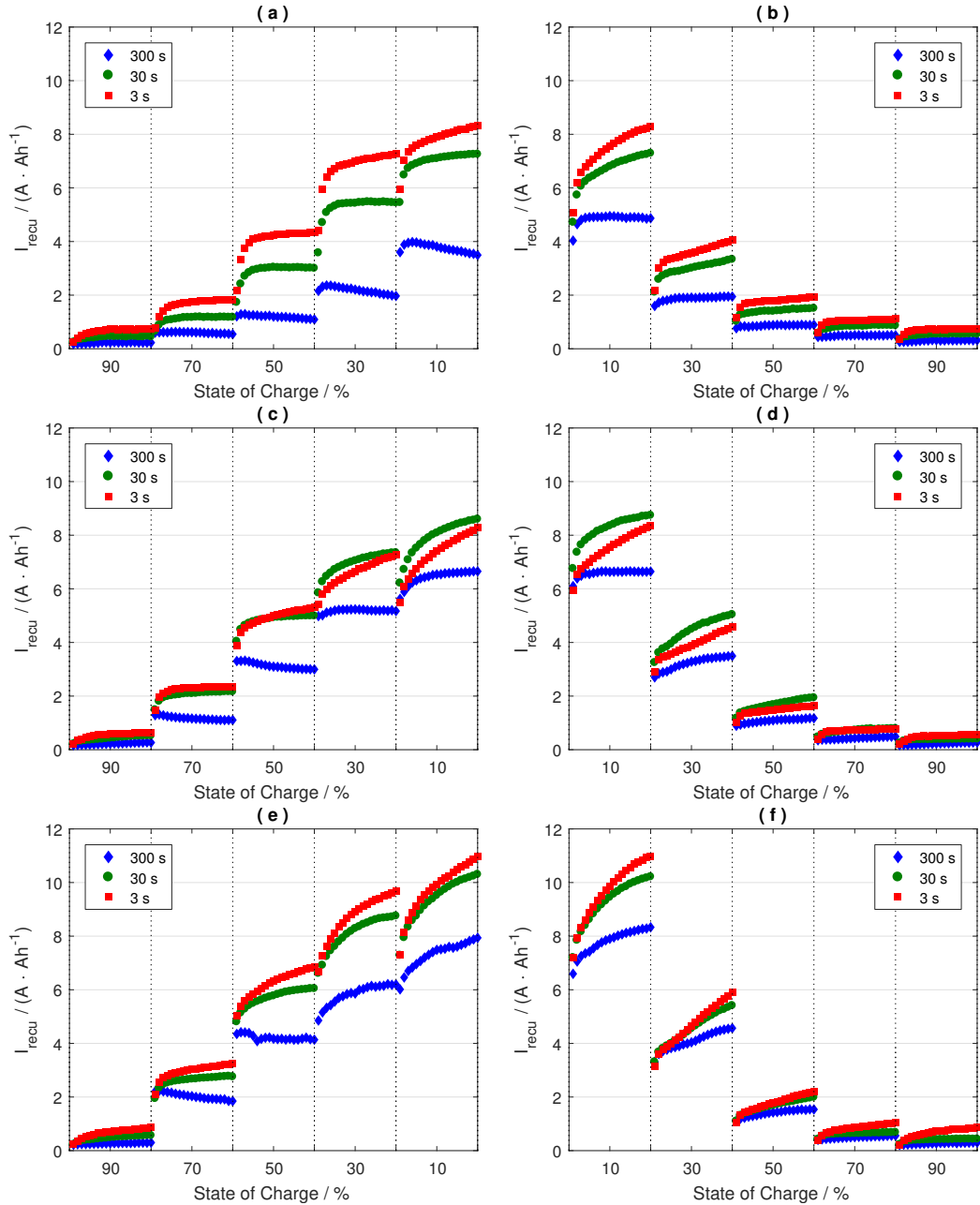

Figure 9: DCA Analysis Result, Increased Current Limit. (a) 0°C with Discharge History, (b) 0°C with Charge History, (c) 25°C with Discharge History, (d) 25°C with Charge History, (e) 40°C with Discharge History, (f) 40°C with Charge History

Also observed previously was that at high currents the rest period which produces the best results is 30 s, in contrast to those results at lower currents where DCA improves with reducing

16

rest period. It may be seen from these results however that this is reversed and the shorter rest periods again yield better DCA performance. Interestingly this is observed at both extremes of temperature.

To confirm the behaviour observed at 25°C, the test was repeated on a second battery, the results of which agree with the previous test at this temperature, indicating the results are valid. This further shows how DCA performance is critically dependant on environmental factors and test conditions.

7.2. Extended Microcycle Testing

A second area of interest is the DCA performance of the cells during the DCAPP period. Analysis of the tests already performed shows that this is not constant across the period, rather DCA is seen to either increase or decrease, apparently dependant on the DCAPP rest period. This behaviour has only been noted due to the presentation of DCA results on a per-microcycle basis, they are more usually shown as the average charge acceptance across the whole DCAPP period, thus obscuring any change during that time.

To investigate this phenomenon, a new test procedure has been designed with the length of the DCAPP increased. A series of tests have been performed using this procedure, the results of which appear highly promising. It has been shown that even with the longer period DCA performance shows significant variation, also the way the results are presented is key to revealing the underlying performance. Initially testing took place using a modified DCAPP consisting of 100 microcycles. This was performed with the cell at 70% SoC and with both charge and discharge history.

Figure 10a shows the analysis result when plotted against microcycle number. From this it appears as if the DCA for all rest periods has essentially stabilised by the end of the 100 pulses, this seems to be true for both charge and discharge history. However it is clear to see from Figure 10b, which shows the same data, but plotted against time, that this is far from true. In fact only the result at 300 s has stabilised, the others continue to show change. Of particular interest are the results with discharge history, here the trend seems to show that the DCA follows a similar profile for all rest periods, but is shifted up with reduced rest. For cells with charge history it is obvious that those with 3 & 30 s rest periods have not stabilised, also they do not appear to be following a common trend — certainly not in the way those with discharge history do.

In light of these results the test was modified such that the DCAPP was applied for a specified period of time, regardless of rest period. In this case the test was run for 60,000 seconds (16.67 hours), which gives around 100 cycles with 300 s rest period, thus allowing for a comparison with the previous test results. The result of this test is given in Figure 10c.

Considering first the results when the cell has charge history, this agrees with that previously observed, in that the responses diverge quite significantly with the two shortest rest periods in-
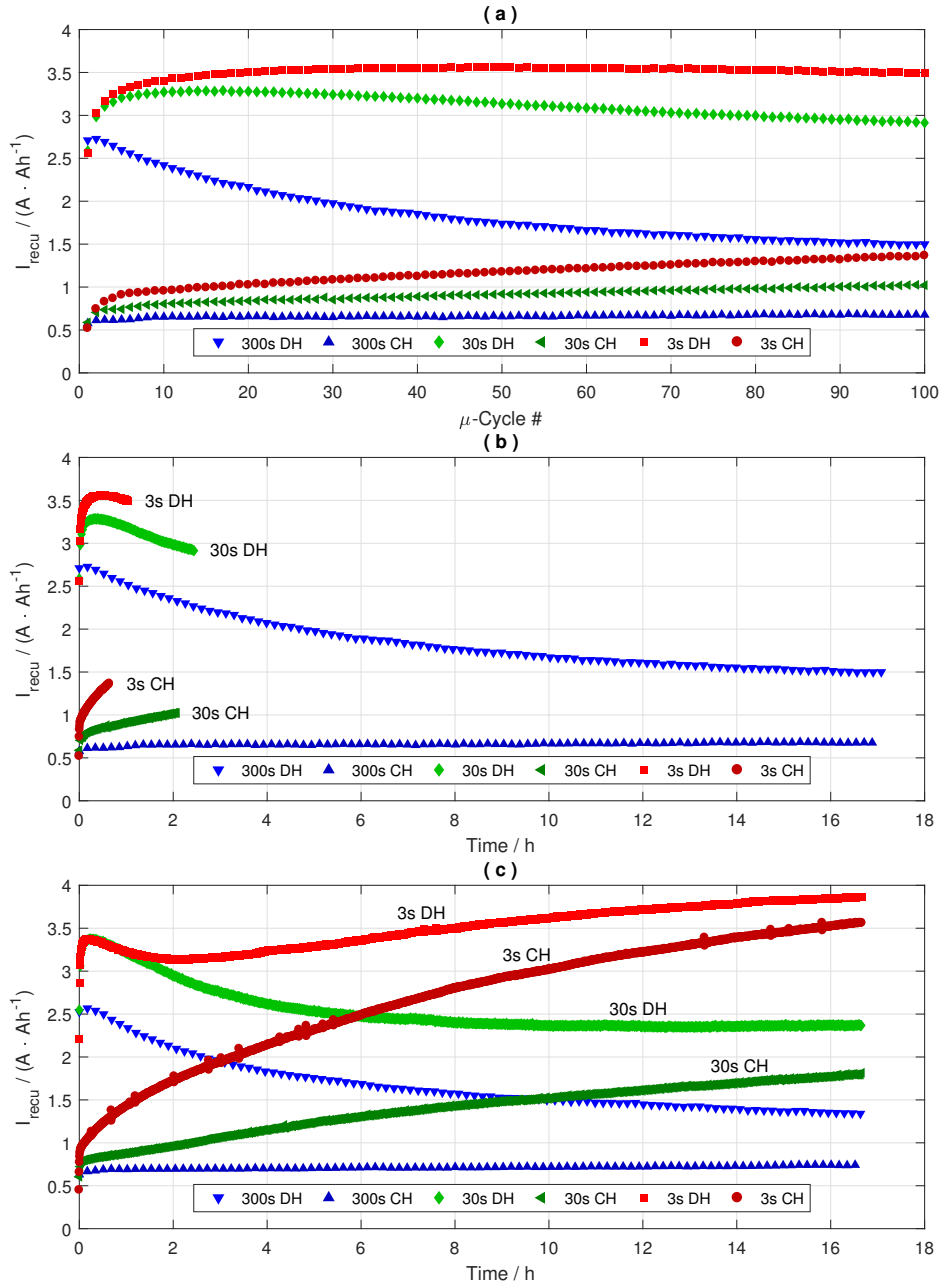
17

Figure 10: DCA Analysis Result, Extended DCAPP at 25°C. (a) against Microcycle #, (b) against Test Time, (c) Test with Constant Time

creasing rapidly. It can also be seen that the increase leads to a convergence between the charge and discharge histories, although even after a significant period of cycling, the results never actually meet. This convergence is also observed with the 300 s rest period, although in this case the result with discharge history reduces to meet that with charge history. Again, the two never meet.

The picture for discharge history is slightly more complex. Initially the results appear to

18

follow those previously observed, with all three rest periods displaying a similar shape, shifted along the y-axis. This remains true for the 300 & 30 s rest periods, which correlate well across the test period. For 3 s rest however, the trend diverges quite significantly from around the 2-hour mark onwards. This divergence is possibly attributable to the increase in cell temperature due to the much higher energy throughput associated with the shortest rest period. As has been previously shown, DCA is partially dependant on temperature, so the effect of this increase must be considered when analysing these results.
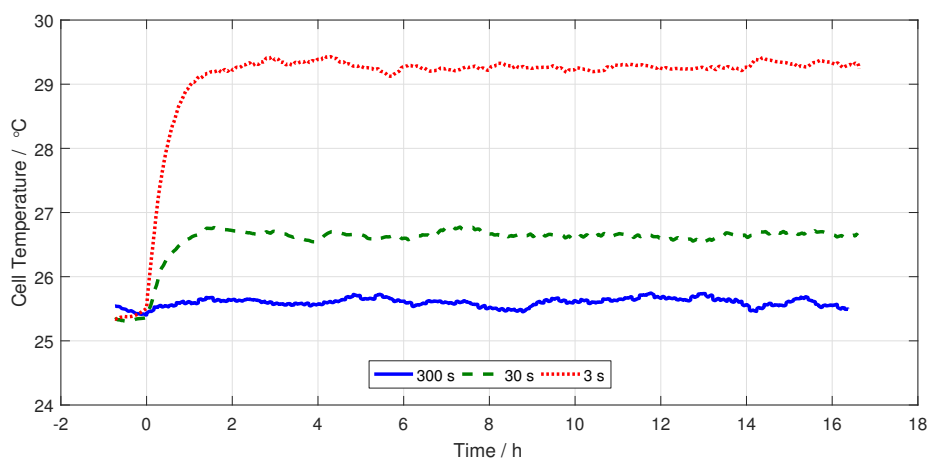

Figure 11: Cell Surface Temperature during Extended DCAPP test, with Discharge History

Figure 11 shows the temperature measured on the surface of the cell for the duration of the tests conducted with both discharge and charge history. It may be seen that during 3 s rest section of the test procedure, the cell temperature rose by around 4°C. The maxima of this rise occurs around 2 hours after the start of the test, at a similar time to when the divergence in DCA performance becomes significant. This may be compared to the temperature increase of around 1°C seen for the equivalent test with 30 s and the negligible increase with 300 s rest periods.

8. Conclusions

Following the testing of carbon-enhanced lead-acid cells carried out over a range of SoC, rest periods and temperatures there is clear correlation between DCA and both SoC and temperature. DCA is improved at higher temperatures and at lower SoC, furthermore there is some evidence to suggest the cells may exhibit a 'memory effect' leading to improved DCA following a period of discharging. It has also been shown that the rest period used within the test regime affects the DCA response of the cells, in all cases reducing the rest period improves charge acceptance. These trends have also been shown to be present in different cell chemistries, although the magnitude of the effects does differ markedly.

19

Secondly the work shows that to select a battery based on DCA performance it is important to consider the range of SoC over which the battery will be operated – picking narrow SoC window to base results on risks missing important changes in performance as SoC varies, which could lead to sub-optimal performance in certain conditions. As an example, from the results obtained, if consistent DCA performance were desired in a system subject to large SoC variations and various charge histories, then LFP would seem the most appropriate. If however operation was to be confined to a small SoC window around 50%, carbon-enhanced lead gives better performance.

A second issue to consider is the magnitude of the recuperation current, especially at low SoC; under these conditions carbon-enhanced lead outperforms the lithium cells. The LFP cell shows a maximum recuperation current of 4 A·Ah^{-1} only at 10% SoC or below. Both of these compare unfavourably to carbon-enhanced lead which reaches 4 A·Ah^{-1} at around 50% SoC and will accept recuperation currents of 6 - 8 A·Ah^{-1} at low SoC.

These tests also show that DCA is not a static parameter, fundamental to the cell. Rather it is critically dependant on environmental conditions, the history of operations performed on the cell and the electrochemical balance within the cell at any given time. In order to properly understand DCA performance a more thorough test procedure is required than that provided by the A3 Test, one that examines the charge acceptance at various SoC and accounts for the effects of charge history.

Acknowledgements

References

[1] P. T. Moseley, D. A. Rand, Partial state-of-charge duty: A challenge but not a show-stopper for lead-acid batteries!, ECS Transactions 41 (13) (2012) 3–16. `doi:10.1149/1.3691907`.

[2] M. Ehsani, Y. Gao, J. M. Miller, Hybrid electric vehicles: architecture and motor drives, Proceedings of the IEEE 95 (4) (2007) 719–728. `doi:10.1109/jproc.2007.892492`.

[3] E. Karden, P. Shinn, P. Bostock, J. Cunningham, E. Schoultz, D. Kok, Requirements for future automotive batteries–a snapshot, Journal of Power Sources 144 (2) (2005) 505–512. `doi:10.1016/j.jpowsour.2004.11.007`.

[4] E. Karden, S. Ploumen, B. Fricke, T. Miller, K. Snyder, Energy storage devices for future hybrid electric vehicles, Journal of Power Sources 168 (1) (2007) 2–11. `doi:10.1016/j. jpowsour.2006.10.090`.

[5] H. Budde-Meiwes, D. Schulte, J. Kowal, D. U. Sauer, R. Hecke, E. Karden, Dynamic charge acceptance of lead–acid batteries: Comparison of methods for conditioning and testing, Journal of Power Sources 207 (2012) 30–36. `doi:10.1016/j.jpowsour.2011.12.045`.

[6] European Committee for Electrotechnical Standardisation, EN 50342-6:2015. Lead-acid starter batteries - Part 6: Batteries for Micro-Cycle Applications (November 2015).

[7] ISOLAB 3a, Development and testing of VRLA cells with optimised grid designs for mild hybrid applications: Accelerated programme to provide batteries for vehicle trials in a Honda Insight (ALABC Project 1012KD), Progress Report (May 2013).

[8] S. Schaeck, A. Stoermer, J. Albers, D. Weirather-Koestner, H. Kabza, Lead-acid batteries in micro-hybrid applications. Part II. Test proposal, Journal of Power Sources 196 (3) (2011) 1555–1560. `doi:10.1016/j.jpowsour.2010.08.079`.

[9] K. Vetter, Elektrochemische Kinetik. (German) *[Electrochemical Kinetics]*, Springer, Berlin, 1961.

[10] C. R. Gould, C. M. Bingham, D. A. Stone, P. Bentley, New battery model and state-of-health determination through subspace parameter estimation and state-observer techniques, Vehicular Technology, IEEE Transactions on 58 (8) (2009) 3905–3916. `doi:10.1109/TVT.2009.2028348`.

[11] A. Fairweather, M. Foster, D. Stone, Modelling of VRLA batteries over operational temperature range using pseudo random binary sequences, Journal of Power Sources 207 (2012) 56–59. `doi:10.1016/j.jpowsour.2012.02.024`.

[12] K. J. Laidler, The development of the Arrhenius equation, J. Chem. Educ 61 (6) (1984) 494. `doi:10.1021/ed061p494`.

[13] T. Sharpe, R. Conell, Low-temperature charging behaviour of lead-acid cells, Journal of Applied Electrochemistry 17 (4) (1987) 789–799. `doi:10.1007/BF01007816`.